

Recovery of contour nodes in interdependent directed networks

Ignacio A. Perez^{1,*} and Cristian E. La Rocca¹

¹*Instituto de Investigaciones Físicas de Mar del Plata (IFIMAR)-Departamento de Física,
FCEyN, Universidad Nacional de Mar del Plata-CONICET,
Deán Funes 3350, (7600) Mar del Plata, Argentina*

Abstract

Extensive research has focused on studying the robustness of interdependent non-directed networks and the design of mitigation strategies aimed at reducing disruptions caused by cascading failures. However, real systems such as power and communication networks are directed, which underscores the necessity of broadening the analysis by including directed networks. In this work, we develop an analytical framework to study a recovery strategy in two interdependent directed networks in which a fraction q of nodes in each network have single dependencies with nodes in the other network. Following the random failure of nodes that leaves a fraction p intact, we repair a fraction of nodes that are neighbors of the giant strongly connected component of each network with probability or recovery success rate γ . Our analysis reveals an abrupt transition between total system collapse and complete recovery as p is increased. As a consequence, we identify three distinct phases in the (p, γ) parameter space: collapse despite intervention, recovery enabled by the strategy, and resilience without intervention. Moreover, we demonstrate our strategy on a system built from empirical data and find that it can save resources compared to a random recovery strategy. Our findings underscore the potential of targeted recovery strategies to enhance the robustness of real interdependent directed networks against cascading failures.

* Correspondence: ignacioperez@mdp.edu.ar

I. INTRODUCTION

Most of real-world systems usually interact with one another through dependencies. For instance, critical infrastructures such as power grids and water supply systems depend on communication networks for operational control, while communication networks require electricity to function and water systems are used to cool power generators. Dependencies can create feedback loops that are not captured by traditional single-network models. Thus, interdependent networks, which have connectivity links within each single network and dependency links between different networks, exhibit structural and dynamical behaviors distinct from isolated systems [1–5]. While interdependencies can enhance the overall performance of networks, they may also introduce vulnerabilities. A small system malfunction can propagate back and forth between two (or more) interdependent systems in a process known as cascading failures [6–9]. Incidents such as the faulty software update from CrowdStrike [10] in July 2024, which led to widespread disruptions of airlines, banks, broadcasters, healthcare providers, etc., hurricane Katrina in USA [11], where oil rigs and refineries were destroyed, causing an exponential rise in the price of fuel, or the massive 2003 blackout in Italy [12], which affected transportation and communications networks, underscore the need for studying collapse in interdependent networks in order to build more robust systems and design effective response strategies. For example, the restoration of electric power systems is particularly critical, as these systems are essential for the operation and management of nearly all other infrastructures. In practice, certain electric transmission substations are often prioritized during recovery efforts because they support critical facilities, such as airports, hospitals, and emergency services. This highlights the importance of effective recovery strategies in minimizing the impact of cascading failures and ensuring the resilience of interconnected systems.

In a pioneering work, Buldyrev et. al. [13] studied cascading failures in two fully interdependent non-directed networks by developing an analytical framework based in node percolation [14, 15], a process extensively used for modeling propagation phenomena. In isolated networks, random node percolation occurs when nodes are removed at random leaving a fraction p intact, producing the network breakdown into clusters of connected nodes with different size. In this process, the giant component (GC), i.e. the cluster of biggest size P_∞ , undergoes a continuous transition at a critical point p_c , which separates

a collapsing phase ($P_\infty = 0$ for $p \leq p_c$) from a non-collapsing phase ($P_\infty > 0$ for $p > p_c$). Buldyrev et. al. found that interdependent systems have larger values of p_c and thus are more fragile than isolated networks, when the degree distribution is the same. Moreover, they found that interdependent networks present abrupt first-order transitions, in which P_∞ changes from a finite value to zero with a small variation of the fraction p of initial remaining nodes.

Several modifications have been made to the original model [13] for non-directed networks to study system robustness [16–24] or with the focus on designing mitigation and recovery strategies [25–27], among other goals. For instance, Di Muro et. al. [28] studied two interdependent networks where failed nodes that are neighbors of the GC of each network are repaired with probability γ . This is a reasonable strategy given the existing facilities to do so in many real systems such as transportation networks, where it is easier to bring the necessary equipment for repairing a damaged site through the transportation system itself. Their results show abrupt transitions between complete collapse ($P_\infty = 0$) and full functionality ($P_\infty = 1$). More precisely, they found three distinct phases: a phase in which the system never collapses without being restored, another phase where breakdown is avoided due to the strategy, and a phase in which system collapse cannot be avoided, even if the strategy is implemented.

While significant progress has been achieved in the study of non-directed systems, research efforts have only recently shifted toward exploring interdependent directed networks. Many real-world systems are inherently directed, such as transportation networks and power grids [29, 30], biological networks [31–34], and the World Wide Web [35], and it is known that directed links (e.g., from generators to substations that lower energy voltage in a power grid) alter network structure and can have a significant effect on failure propagation [36–38]. Thus, research on interdependent directed networks has initially focused on studying the robustness of systems under different types of failures or topologies [39–42]. We believe that, in addition, it is necessary to explore mitigation or recovery strategies that can help to develop more resilient interdependent directed systems against cascading failures.

In this work, we model a process of cascading failures in an interdependent system composed of two directed networks, where a fraction q of nodes in each network have single dependencies with nodes from the other network. Inspired by the work in [28], we implement a recovery strategy where a subset of the nodes belonging to the contour of the

giant strongly connected component (GSCC) of each network are repaired with probability γ . This probability can be interpreted as the technical ability to repair nodes or the rate of success, in the best-case scenario where resources are always available. Using random node percolation and generating functions, we develop an analytical approach to compute the size of the mutual giant strongly connected component (MGSCC), P_∞ , at the end of the process, after an initial random failure of a fraction $1 - p$ of nodes in one of the networks. Moreover, we build phase diagrams for P_∞ on the plane (p, γ) , which allow us to recognize different system behaviors. In addition, we simulate the process on a system built from empirical data and contrast the proposed strategy with the random recovery of nodes, in order to demonstrate the practical application of our model in a realistic scenario and the advantages with respect to other known recovery strategies.

II. MODEL

Our system consists in two interdependent directed networks A and B with the same size N . Within each network or layer, nodes are connected via directed connectivity links, where $P_i^{in}(k_i^{in})$ and $P_i^{out}(k_i^{out})$, $i = A, B$, are the uncorrelated degree distributions for incoming and outgoing links and $k_{in/out}$ represents the number of incoming/outgoing links that a node can have in network i . To build a given layer, we use a slight variation of the configuration model [36, 43, 44] with the condition $\langle k_{in} \rangle = \langle k_{out} \rangle$ (see Appendix A). The structure of a directed network can be mainly described by the following three components that add to the giant weakly connected component (GWCC), the largest cluster where each node can reach any other node in the cluster by following one path ignoring link directions [37]:

1. Giant strongly connected component (GSCC): The largest component of connected nodes where each node can reach any other node in the cluster by following one directed path. In the process of cascading failures, we regard the GSCC as the functional component within each network.
2. Giant in-component (S^{in}): Contains nodes that can reach the GSCC by following a directed path.
3. Giant out-component (S^{out}): Contains nodes that can be reached from the GSCC by following a directed path.

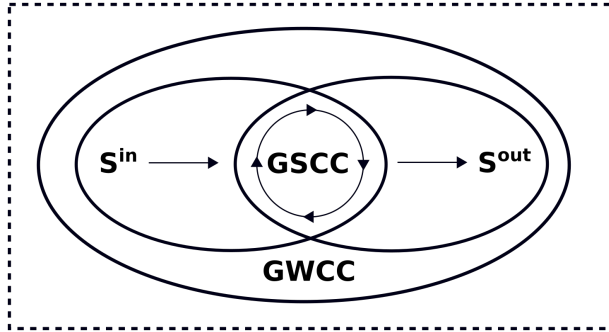


FIG. 1. Scheme of the structure of directed networks. A giant weakly connected component (GWCC) arises, where nodes can reach other nodes through paths that ignore directions. Within this component, a smaller but strongly connected component (GSCC) contains nodes that can follow a directed path to every other node in the component. Thus, closed paths of directed links form between each pair of nodes in the GSCC. Then, nodes that can arrive to the GSCC through directed paths belong to the S^{in} component, while nodes reached from the GSCC via directed paths belong to the S^{out} component.

By definition, the GSCC is contained in both S^{in} and S^{out} , $GSCC = S^{\text{in}} \cap S^{\text{out}}$. These components are illustrated in Fig. 1.

Once connectivity links within each network are set, we build the interdependencies between networks by imposing a fraction q_A of nodes in network A to depend on nodes from network B and a fraction q_B of B-nodes to depend on A-nodes, in the following manner:

1. A-nodes (B-nodes) with dependencies depend only on a single, randomly selected B-node (A-node).
2. If different A-nodes (B-nodes) have dependencies, these dependencies correspond to different B-nodes (A-nodes).
3. If node i from A (B) depends on node j from B (A), and if node j depends on node k from A (B), then $i = k$ (known as the no-feedback condition [13, 45]).

In this way, dependencies can be unidirectional or bidirectional, the latter of which are allowed by condition 3. It is important to note, as we state in Appendix A, that for the internal connectivity links within each network there are no bidirectional connections.

At time step $t = 0$, we start the cascading failures by assuming that a random fraction $1 - p$ of nodes in layer A fail, and we remove these nodes. This causes the fragmentation

into GSCC_A , which remains functional, and finite clusters (FC_A), which we consider to malfunction as they stop receiving enough support from their own network because they lose connection with the GSCC_A . Thus, finite clusters are removed too. A fraction q_B of the total removed nodes in A cease to provide support to the same fraction of nodes in layer B, causing its fragmentation into GSCC_B and FC_B . Again, we assume that finite clusters in B fail. Hereafter, the failures that will pass from one network to the other will only be due to finite clusters. In Fig. 2, we show a scheme of the process for a small system. At the end of the process, P_∞^A and P_∞^B are the fractions of nodes in GSCC_A and GSCC_B , respectively. The union of these components make up the MGSCC, of size $P_\infty = (P_\infty^A + P_\infty^B)/2$, as long as both components have a finite size different from zero and they are interconnected through dependency links (Fig. 2 (a)). Otherwise, $P_\infty = 0$ (Fig. 2 (b)). If the cascade evolves without any kind of intervention, there is a critical point p_c below which the interdependent directed networks collapse, i.e. $P_\infty = 0$ for $p \leq p_c$ [39]. As observed in [39], and similar to non-directed interdependent networks [16], the transition at p_c changes from second-order to first-order as the coupling between networks is decreased.

Therefore, in order to mitigate the damage in the system, or either delay or avoid its collapse, we immediately implement a recovery strategy in both networks. The strategy consists in repairing, with probability γ , a subset of nodes from the ‘‘contour’’ or perimeter C_i of GSCC_i , $i = A, B$. A node from layer i belongs to C_i if it is a failure and has, at least, one incoming and one outgoing link that lead to GSCC_i . The contour nodes that we consider for repairing may fulfill any of the following conditions:

1. Nodes which have no dependencies and that do not support any node in the other network.
2. Nodes with dependencies, for which we also check if their dependencies are contour nodes in the other layer. If that is the case, we repair both nodes. If the second node belongs to the GSCC of its corresponding layer, then we just recover the first node.
3. Nodes which do not have dependencies but support nodes in the other network, excluding the case where the second node is a contour node. In this case, we only repair the first node.

The restoring of a node implies that it turns back to a functional state and all of its links with the GSCC become available again. Note that, in this way, we can preserve the original degree

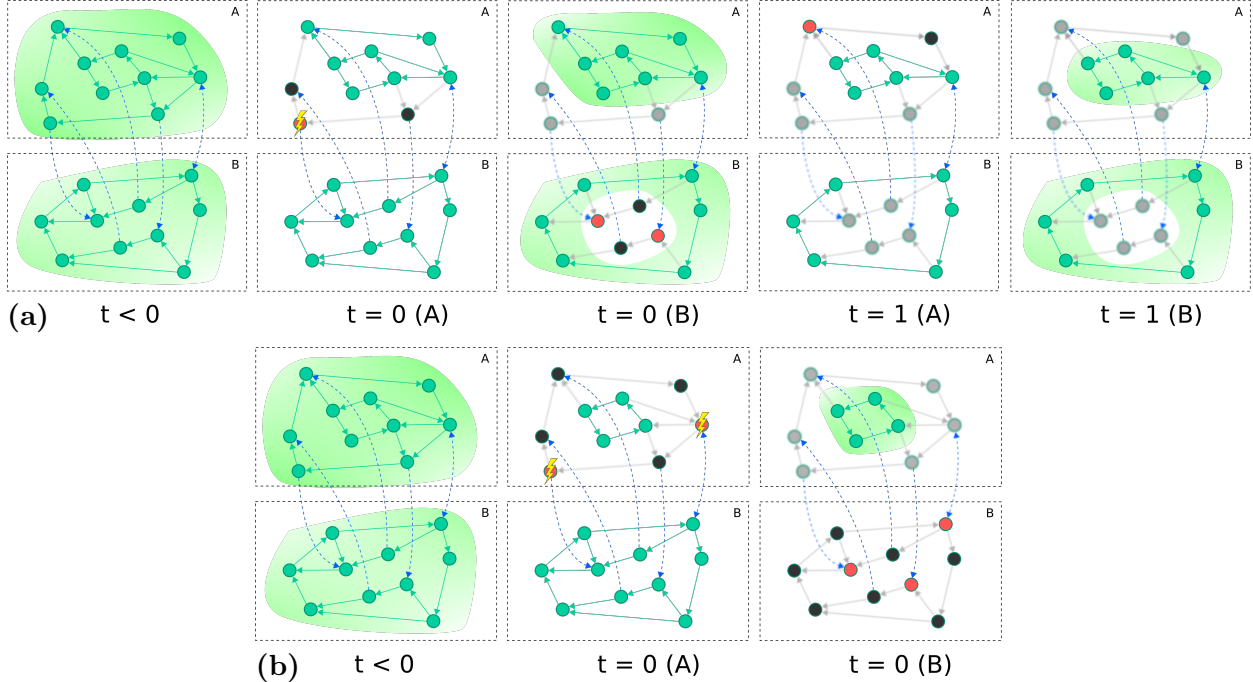


FIG. 2. Cascading failures in two networks of size $N = 10$ and $q_A = q_B = 0.3$. At each time step, events occur first in network A and then propagate to network B. (a) At $t < 0$, the GSCC of each network is highlighted with a light green shadow. At $t = 0$, a node is struck by lightning and fails ($1 - p = 0.1$). As a result, the two black nodes turn into finite clusters and fail, as they get disconnected from the GSCC_A . Two of the three A-failures propagate to B through dependencies (dashed lines). These B-failures are highlighted in red. Then, network B fragments into GSCC_B and finite clusters (black nodes), the latter of which cause subsequent failures in A. At $t = 1$, network A fragments and the cascade stops since failures from finite clusters in A cannot propagate to B. The size of the MGSCC is $P_\infty = (P_\infty^A + P_\infty^B) = (0.5 + 0.6)/2 = 0.55$. (b) Initially, two nodes fail in network A ($1 - p = 0.2$) producing fragmentation into GSCC_A and finite clusters (black nodes). Failures spread to B and completely eliminate the GSCC_B . The cascade stops at $t = 0$ as finite clusters in B do not provide support to any functional A-node. The size of the MGSCC is $P_\infty = 0$, since $P_\infty^B = 0$.

distributions in both networks, since we use already existing links to recover contour nodes. Therefore, we are able to map our model directly with the process of node percolation [37, 39].

Finally, after applying the strategy, we increase time in one unit and propagate the failures from the finite clusters FC_B back to network A, taking into account the fraction q_A of nodes in A that have dependencies. The time step $t > 0$ includes the failure of nodes in A due to

dependencies with nodes in FC_B at $t - 1$, the subsequent propagation of failures from FC_A to layer B, and the implementation of the recovery strategy in both layers. This process of cascading failures with recovery continues until a stationary state is reached, which depends on the values of p , q_A , q_B , and γ , where there are no more failures and neither contour nodes available to repair.

III. ANALYTICAL RESULTS AND SIMULATIONS

In the following, we develop a theoretical approach to describe the model introduced in the previous section by establishing an equivalent process of node percolation and using the generating functions $G_{0i}^{in}(x) = \sum_{k_i^{in}} P_i^{in}(k_i^{in})x^{k_i^{in}}$ and $G_{0i}^{out}(x) = \sum_{k_i^{out}} P_i^{out}(k_i^{out})x^{k_i^{out}}$, $i = A, B$, which generate the self and mutually uncorrelated degree distributions $P_i^{in}(k_i^{in})$ and $P_i^{out}(k_i^{out})$, respectively. Let $p_i(t)$ be the effective fraction of remaining nodes in network i at time t , before applying the recovery strategy. Given that the in-degree is not correlated with the out-degree, the fraction of nodes belonging to the $GSCC_i$ is [37]

$$P_\infty^i(t) = p_i(t) g_i(p_i(t)), \quad g_i(x) = (1 - G_{0i}^{in}(1 - f_\infty^{in}(x)))(1 - G_{0i}^{out}(1 - f_\infty^{out}(x))),$$

where f_∞^{in} (f_∞^{out}) represents the probability of starting from a randomly chosen link in network i and moving only against (along) the edge directions to arrive to the S_i^{out} (S_i^{in}) component (remember Fig. 1). The probabilities f_∞^{in} and f_∞^{out} satisfy the transcendental equations

$$\begin{aligned} f_\infty^{in} &= x(1 - G_{1i}^{in}(1 - f_\infty^{in})), \\ f_\infty^{out} &= x(1 - G_{1i}^{out}(1 - f_\infty^{out})), \end{aligned} \tag{1}$$

where G_{1i}^{in} and G_{1i}^{out} are the generating functions of the number of incoming links arriving at a node reached by moving against the direction of a randomly chosen link and the number of outgoing links leaving a node reached by moving along the direction of a randomly chosen link, respectively [37].

Recall that the cascading failures start, at time $t = 0$, with the random removal of a fraction of A-nodes, denoted by $1 - p$. The remaining fraction of nodes in A is $p_A(0) = p$, where a fraction $FC_A(0) = p_A(0) - P_\infty^A(0) = p(1 - g_A(p))$ of those nodes corresponds to finite clusters. Then, the remaining fraction of nodes in B is $p_B(0) = 1 - q_B(1 - P_\infty^A(0)) =$

$1 - q_B(1 - pg_A(p))$, since initial failures in A and finite clusters both affect network B, at the beginning, through dependencies. The corresponding size of the finite clusters in B is $FC_B(0) = p_B(0) - P_\infty^B(0)$. At this point of each time step, once the cascade propagates from A to B, we apply the recovery strategy described in the *Model* section.

In order to implement our strategy, we need to find an expression for the fractions $C_A(t)$ and $C_B(t)$ of nodes that belong to the contour of GSCC_A and GSCC_B , respectively. Take, for instance, the fraction $1 - p_A(t)$ that accounts for failed nodes in network A due to node percolation, at time t . We should multiply this by the probability $(1 - G_{0A}^{in}(1 - P_\infty^A(t)))$ that a randomly chosen node has, at least, one incoming link from a node that belongs to the GSCC_A and the probability $(1 - G_{0A}^{out}(1 - P_\infty^A(t)))$ that it has, at least, one outgoing link leading to a node in the GSCC_A . A similar reasoning holds for network B, yielding the fractions of contour nodes in each layer

$$C_A(t) = (1 - p_A(t))(1 - G_{0A}^{in}(1 - P_\infty^A(t)))(1 - G_{0A}^{out}(1 - P_\infty^A(t))), \quad (2)$$

$$C_B(t) = (1 - p_B(t))(1 - G_{0B}^{in}(1 - P_\infty^B(t)))(1 - G_{0B}^{out}(1 - P_\infty^B(t))). \quad (3)$$

Then we update the relative sizes of GSCC_A and GSCC_B due to the recovery of a subset of contour nodes from each network, with probability γ ,

$$\begin{aligned} \overline{P_\infty^A}(t) = P_\infty^A(t) + \gamma & \left[(1 - q_A)(1 - q_B)C_A(t) + \frac{q_A(1 - q_B)C_A(t)C_B(t)}{1 - P_\infty^A(t)} + \frac{q_B C_A(t)C_B(t)}{1 - P_\infty^A(t)} + \right. \\ & \left. + \frac{(1 - q_A)q_B C_A(t)(1 - P_\infty^B(t) - FC_B(t) - C_B(t))}{1 - P_\infty^A(t)} \right], \end{aligned} \quad (4)$$

$$\begin{aligned} \overline{P_\infty^B}(t) = P_\infty^B(t) + \gamma & \left[(1 - q_A)(1 - q_B)C_B(t) + \frac{q_A(1 - q_B)C_A(t)C_B(t)}{1 - P_\infty^A(t)} + \frac{q_B C_A(t)C_B(t)}{1 - P_\infty^A(t)} + \right. \\ & \left. + \frac{(1 - q_B)q_A C_B(t)(1 - P_\infty^A(t) - C_A(t))}{1 - P_\infty^A(t)} \right], \end{aligned} \quad (5)$$

where $\overline{P_\infty^i}(t)$ is the new relative size of GSCC_i , $i = A, B$. Before continuing with the next step, we look at Eq. (4) for layer A to understand the meaning of each term inside the square brackets, for which we include useful diagrams in Fig. 3:

- $(1 - q_A)(1 - q_B)C_A(t)$: Nodes belonging to the contour of GSCC_A that have no dependencies on B-nodes and do not support any B-nodes (Fig. 3 (a)).
- Nodes in C_A that are interconnected with nodes in C_B (Fig. 3 (b)):

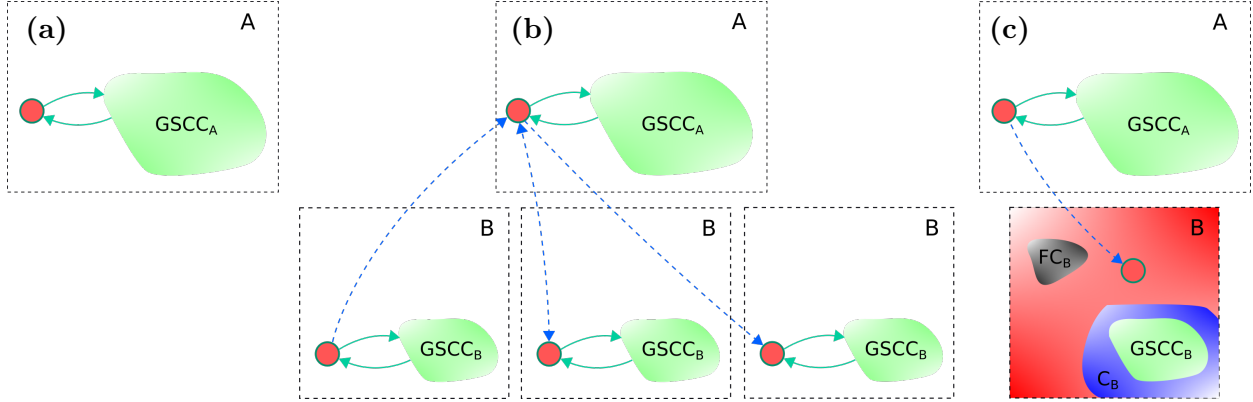


FIG. 3. Scheme of the salvageable contour nodes. We focus on the nodes that can be recovered in network A, according to Eq. (4). Note that single red nodes, both in A and B, belong to the corresponding contour of each network, as they have one incoming and one outgoing link that connects them to the GSCC (they may have more connections with the GSCC). In (a), we show the contour nodes in network A that do not have dependencies and do not support any B-nodes. The diagram in (b) shows the different possibilities for contour nodes in A connected through dependencies with contour nodes in B. The last two instances are represented by the term $q_B C_A(t) C_B(t)$ in Eq. (4). In (c), we show the case in which contour nodes in A provide support to failed B-nodes.

- $q_A(1 - q_B)C_A(t)C_B(t)$: Nodes in C_A that depend on nodes from C_B but do not provide support to them. When the strategy is not applied, this kind of dependencies do not exist because contour nodes in B always depend on failures from A that may belong to C_A or not. However, when the strategy is applied, the recovery of contour nodes may turn some failures in the perimeter of C_A and C_B into new contour nodes, which are considered for repair in the next time step. Thus, while this case is absent at $t = 0$, we must consider it for any other time.
- $q_B C_A(t) C_B(t)$: Nodes in C_A that provide support to nodes in C_B , whether or not the C_A nodes depend on the same C_B nodes.

Note that these two terms involve contour nodes from both networks. As nodes are recovered both in A and B, the terms are present as well in Eq. (5) for network B.

- $(1 - q_A)q_B C_A(t)(1 - P_\infty^B(t) - FC_B(t) - C_B(t))$: Nodes from C_A that do not depend on B-nodes but provide support to failures from network B (Fig. 3 (c)). Note that

we subtract the finite clusters $FC_B(t)$ from the total failures $1 - P_\infty^B(t)$ because, by definition, finite clusters in B are functional right after failures propagate from A to B, and then fail due to being disconnected from the $GSCC_B$. Thus, they cannot depend on failed A-nodes. We also exclude nodes from C_B as we have already considered this case in the term $q_B C_A(t) C_B(t)$.

To complete the description, note that all terms inside the square brackets involving dependencies are conditioned by the probability that dependencies can be established between the corresponding nodes, which is in all cases $1 - P_\infty^A(t)$. The possibilities for network B, reflected on Eq. (5), are similar to those in A with an exception in the last term, $(1 - q_B) q_A C_B(t) (1 - P_\infty^A(t) - C_B(t))$, where it is not necessary to subtract the finite clusters $FC_A(t)$ to the total failures $1 - P_\infty^A(t)$ because finite clusters in A are conformed before $C_B(t)$ and, thus, nodes in FC_A can depend on failed nodes.

Once we update the sizes of $GSCC_A$ and $GSCC_B$, we need to compute the effective fractions of remaining nodes in each network after the application of the strategy, $\overline{p}_A(t)$ and $\overline{p}_B(t)$, by solving the transcendental equations

$$\begin{aligned}\overline{p}_A(t) g_A(\overline{p}_A(t)) &= \overline{P}_\infty^A(t), \\ \overline{p}_B(t) g_B(\overline{p}_B(t)) &= \overline{P}_\infty^B(t).\end{aligned}\tag{6}$$

After this step, we propagate the cascade back to network A through failures in FC_B and we start a new time step. The remaining fractions of nodes before the implementation of the recovery strategy are, at time $t > 0$,

$$p_A(t) = \overline{p}_A(t-1) \left(1 - \frac{FC_B(t-1) \left[q_A q_B + q_A (1 - q_B) \overline{P}_\infty^A(t-1) \right]}{1 - q_B (1 - \overline{P}_\infty^A(t-1))} \right),\tag{7}$$

$$p_B(t) = \overline{p}_B(t-1) \left(1 - \frac{FC_A(t) \left[q_A q_B + q_B (1 - q_A) \overline{P}_\infty^B(t-1) \right]}{1 - q_A (1 - \overline{P}_\infty^B(t-1))} \right),\tag{8}$$

where

$$FC_A(t) = \overline{P}_\infty^A(t-1) - FC_B(t-1) \left[q_A q_B + q_A (1 - q_B) \overline{P}_\infty^A(t-1) \right] - P_\infty^A(t),\tag{9}$$

$$FC_B(t) = \overline{P}_\infty^B(t-1) - FC_A(t) \left[q_A q_B + q_B (1 - q_A) \overline{P}_\infty^B(t-1) \right] - P_\infty^B(t),\tag{10}$$

are the relative sizes of the finite clusters in layer A and B, respectively. In Appendix B, we make a brief comment on how we compute $FC_A(t)$ and $FC_B(t)$. Note that the fractions of

failures that we subtract from each GSCC in Eqs. (9)-(10) are the same fractions that we use in Eqs. (7)-(8) to propagate failures between networks. However, to extend the failures outside the GSCC_A and into $\overline{p}_A(t-1)$, when transmitting failures from FC_B to network A in Eq. (7), we must normalize the failures by leaving aside failed A-nodes that provide support to nodes in B, as these nodes could never be connected to the FC_B . This condition is represented by the denominator $1 - q_B(1 - \overline{P}_\infty^A(t-1))$. In a similar way, we obtain Eq. (8) for p_B .

Based on this analytical approach, we focus on studying the relative size of the MGSCC at the final stage of the process, P_∞ , which is the principal magnitude to reflect the degree of robustness of the interdependent directed networks. The MGSCC includes the A-nodes that belong to GSCC_A and the B-nodes in GSCC_B when the two components are interconnected through dependencies that are set in both ways, i.e. there are nodes in GSCC_A that depend on nodes from GSCC_B and vice-versa. In this case, the relative size of the MGSCC is $P_\infty = (P_\infty^A + P_\infty^B)/2$, where P_∞^A and P_∞^B are the non-zero relative sizes of GSCC_A and GSCC_B at the steady state, respectively. Otherwise, each layer would be isolated from the other one and the system would lose its original integration and functionality, yielding $P_\infty = 0$. In Fig. 4, we show P_∞ as a function of p for two interdependent directed networks with degree distributions $P_A^{in}(k_A^{in} = k) = P_A^{out}(k_A^{out} = k) = P_B^{in}(k_B^{in} = k) = P_B^{out}(k_B^{out} = k) \equiv P(k)$, with $P(k)$ corresponding to (a) an Erdős-Rényi (ER) network and (b) a Scale Free network with exponential cutoff (SFc), and for different fractions of nodes with dependencies $q_A = q_B \equiv q$. We observe that the analytical results (dashed lines) are in well agreement with the results from the simulations, which we represent with different symbols. Our results for $\gamma = 0$ are consistent with those in [39] where, in the absence of a recovery strategy, the critical point p_c becomes smaller as the fraction of interdependent nodes q decreases, which makes the system more robust to cascading failures although less interconnected. This behavior is generalized, in our model, to the scenario where a recovery strategy is implemented ($\gamma > 0$). One of the most significant result that we can extract from Fig. 4 is that the robustness of the system improves when we implement the recovery strategy and for increasing values of γ , to a greater or lesser extent. We observe that this effect on p_c appears to be stronger in absolute terms when the fraction of nodes with dependencies in both networks is $q = 1$ (Fig. 4 (b) and (d)) although, in this case, the failures produce a greater damage to the system compared to the case where $q = 0.5$ (Fig. 4 (a) and (c)). In order to understand

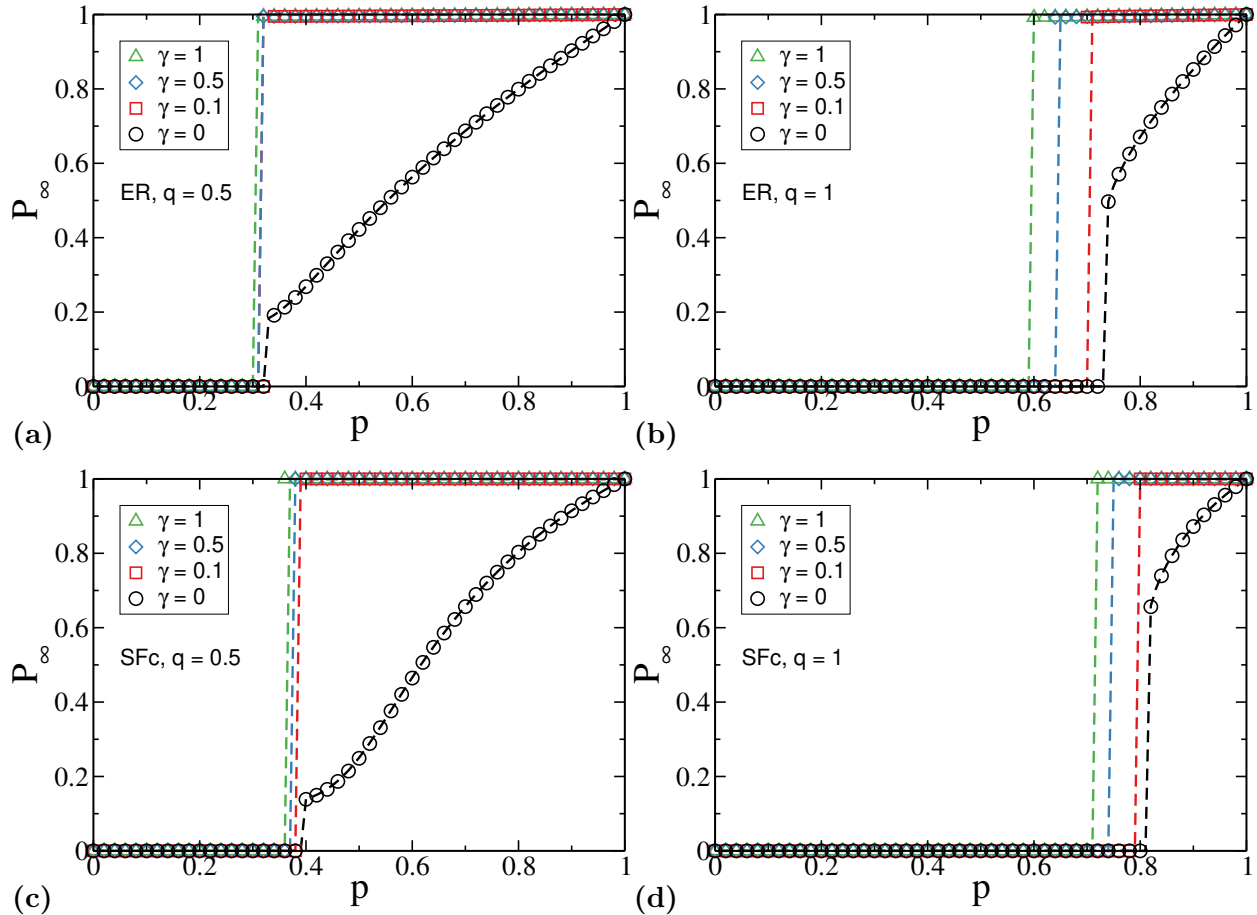


FIG. 4. Outcome of the recovery strategy. The analytical results (dashed lines) of the fraction of nodes in the MGSCC, P_∞ , as function of the fraction of initial remaining nodes $p = p_A(0)$ in network A show a good agreement with the simulations (symbols) for the different values of γ and q . We include the case $\gamma = 0$ as a reference. In (a) and (b), $P(k)$ corresponds to an ER network with $\langle k \rangle = 4$, $k_{min} = 1$, and $k_{max} = 20$. In (c) and (d), we use a SF distribution with $\lambda = 2.35$, exponential cutoff $k_{cut} = 50$, $k_{min} = 2$, and $k_{max} = \sqrt{N}$, which yields $\langle k \rangle \approx 4$. In all cases, for the simulations we build networks of size $N = 10^6$ and we average results over 10^3 realizations.

this behavior, in Fig. 5 we plot the initial fractions of salvageable contour nodes in each network, $\overline{P_\infty^i}(0) - P_\infty^i(0)$, $i = A, B$. We observe that these fractions are larger for the fully interdependent directed networks, i.e. for $q = 1$, at the critical point $p_c(\gamma = 0)$ (dashed line in Fig. 5 (b)), than for the case $q = 0.5$. Besides, for $q = 0.5$, salvageable contour nodes in A rapidly vanish as p falls below $p_c(\gamma = 0)$ (dashed line in Fig. 5 (a)), which limits the possibility of starting a recovery process that leads to the complete restoring of the system.

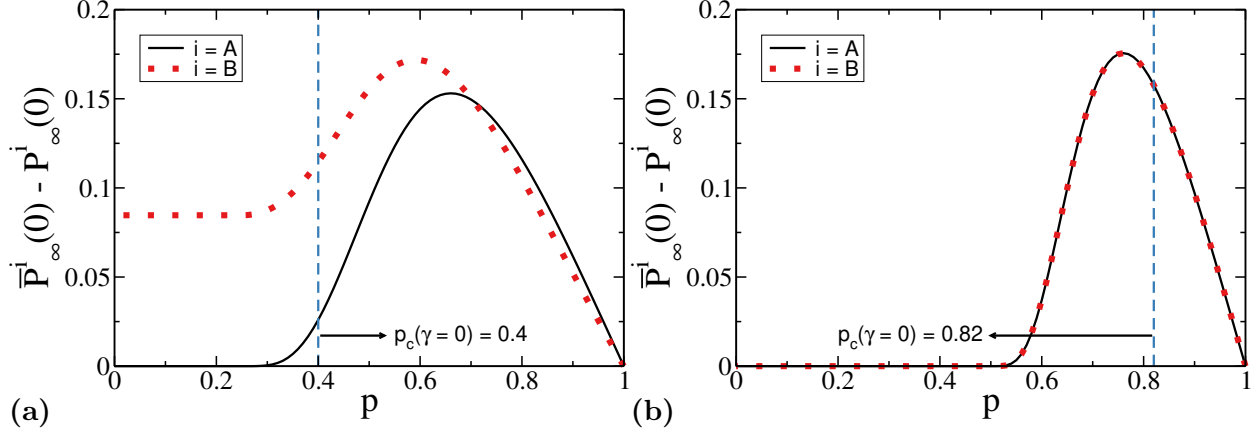


FIG. 5. Fractions of salvageable contour nodes in each network, $\bar{P}_\infty^i(0) - P_\infty^i(0)$, as functions of $p = p_A(0)$ for (a) $q = 0.5$ and (b) $q = 1$. We compute these fractions from Eqs. (4)-(5) with $\gamma = 1$, for the interdependent directed networks presented in Fig. 4 (c) and (d), which present a SFc degree distribution $P(k)$. The dashed lines mark the corresponding critical points in the absence of the recovery strategy ($\gamma = 0$).

The initial size of GSCC_1 , after the first step of the cascade, plays a role too. In this case, it also yields bigger values for the fully interdependent directed networks, but there could be intermediate scenarios where the outcome of the balance between these magnitudes shows an opposite behavior, i.e. the decrease of the interval where the strategy achieves to avoid the collapse of the system as q becomes larger.

Moreover, we observe that the system either collapses ($P_\infty = 0$) or its functionality is completely restored ($P_\infty = 1$) when we apply the recovery strategy, i.e. for $\gamma > 0$. As the process evolves, if there is a step at which failures no longer propagate and a MGSCC still survives, we continue with the recovery of the salvageable contour nodes in each network until we are unable to repair any more. It is crucial for accomplishing the full restoring of the system to repair contour nodes which do not have dependencies and do not support other nodes, in addition to contour nodes which have dependencies and/or are supporting nodes themselves. In this way, the critical point p_c for $\gamma > 0$ corresponds to the threshold for the abrupt transition between a collapsing phase, where $P_\infty = 0$ for $p \leq p_c$, and a completely functional phase, where $P_\infty = 1$ for $p > p_c$. This characteristic is shared with the non-directed model [28].

Finally, regarding the topology of the interdependent directed networks, Fig. 4 shows

that the homogeneous systems (Fig. 4 (a) and (b)), are more robust when compared to heterogeneous systems (Fig. 4 (c) and (d)) with the same average degree. The lower values for p_c in systems with ER degree distributions are observed for all the values of q and also for all the values of the recovery probability γ . These results agree with those obtained in non-directed models [13, 16, 46].

In order to analyze the overall robustness of the system and the degree of difficulty with which it can be restored, we compute the phase diagrams in the plane (p, γ) for the interdependent directed networks analyzed above. A possible approach to do this is by means of the number of iterations (NOI) that the system requires to reach the steady state. In other words, the NOI accumulates the iterative steps (discrete time t), each one of which can comprehend the propagation of failures and the implementation of the recovery strategy or only one of these processes, until the system collapses or gets completely restored. In this way, the NOI is a measure of the velocity of the process and it is known that, if no recovery strategy is applied, it shows a peak in the vicinity of criticality [46], revealing a slow dynamic behavior. Thus, the number of steps necessary for the system to reach the steady state increases significantly when p is close to p_c , but away from criticality only a few steps are required. Therefore, the NOI can be used as an accurate measure for computing the critical threshold p_c for each value of γ . In Fig. 6, we show the NOI obtained from the theoretical approach for the homogeneous networks presented earlier (see Fig. 4 (a) and (b)), which is enough to demonstrate the qualitative behavior of this magnitude for our process. In Figs. 6 (a) and (b) for $q = 0.5$ and $q = 1$, respectively, we see that there is a peak that signals the criticality if we implement the recovery strategy, although it is not as sharp as for the case $\gamma = 0$ (see the inset in Fig. 6 (b)). Above the critical point, for $p > p_c$, the NOI appears to decrease in a constant manner, opposed to the abrupt way in which the NOI increases as we get close to p_c from below. In addition, the curves obtained for the different values of γ shows us that the number of steps that the system requires to reach the steady state decreases as the fraction of recovered nodes becomes larger. Measuring the position of the maximum value in the NOI can involve extensive data analysis, as observed in the number of steps that the process can last from Fig. 6 (a). For this reason, we appeal to an equivalent method for analytically computing the phase diagrams, which is also used for the non-directed model [28]. Given a fixed value of p , we run the theoretical model for decreasing values of the probability of recovery γ until the size of the MGSCC falls to zero.

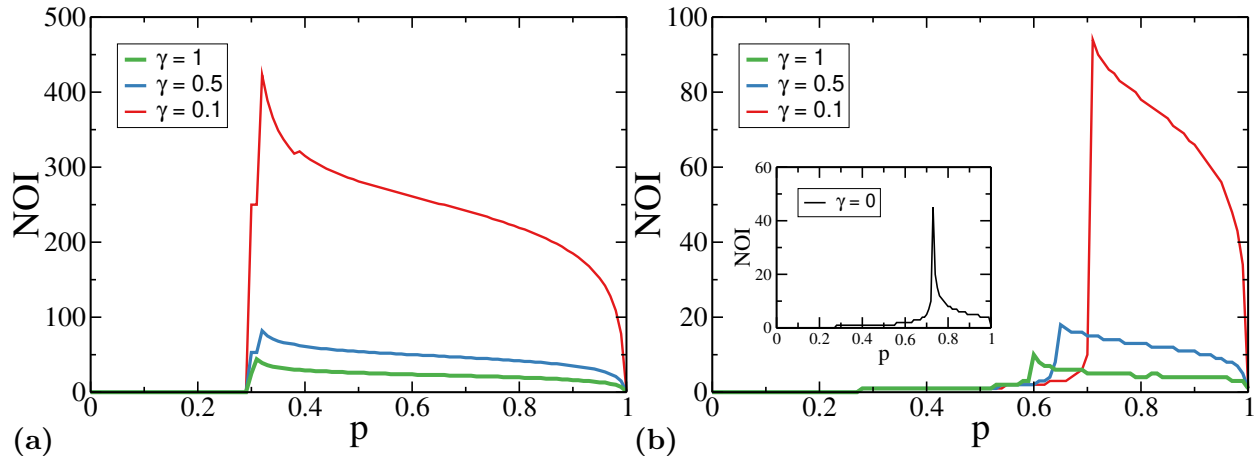


FIG. 6. Number of iterations (NOI) as function of $p = p_A(0)$, for the interdependent directed networks analyzed in Fig. 4 (a) and (b), which present an ER degree distribution $P(k)$. Results in (a) correspond to $q = 0.5$, while in (b) $q = 1$. The thickness of the curves increase with the value of the recovery probability γ . We included an inset in (b) for the case $\gamma = 0$, which shows the typical sharp peak at criticality.

We record the value of γ for which this occurs as $\gamma_c(p)$ and we find, in all cases, that this value is the same that we obtain by measuring the peak of the NOI.

In Fig. 7, we show the phase diagrams for the interdependent directed networks that we analyzed earlier (see Fig. 4). Each one of the curves (solid lines) corresponds to a different value of q and represents the critical value of the recovery probability, $\gamma_c(p)$, such that the system collapses for $\gamma \leq \gamma_c$ ($P_\infty = 0$ in region I). Otherwise, if the strategy is sufficiently effective, i.e. $\gamma > \gamma_c$, the system is completely restored ($P_\infty = 1$). In this case, we differentiate two regions for clarity. The curve $\gamma_c(p)$ decreases as we increase the value of p , until it reaches zero at a given point. This point corresponds to the critical threshold in the absence of a strategy, i.e. $p_c(\gamma = 0)$ such that $P_\infty(p_c(\gamma = 0)) = 0$. If we continue increasing the value of p , the size of the MGSCC at the end of the process becomes different from zero and starts increasing, regardless of the effectiveness of the recovery strategy. In this region of the diagram, the implementation of our strategy is not crucial to avoid the collapse of the system. The dashed lines in Fig. 7 mark the beginning of this region (region II, where $P_\infty > 0$ for $\gamma = 0$ and $P_\infty = 1$ for $\gamma > 0$). Within the remaining area, delimited by the curves $\gamma_c(p)$ and $p = p_c(\gamma = 0)$, our strategy achieves the most relevant results, avoiding total breakdown ($P_\infty = 0$ for $\gamma = 0$) and recovering the functionality of the system in its

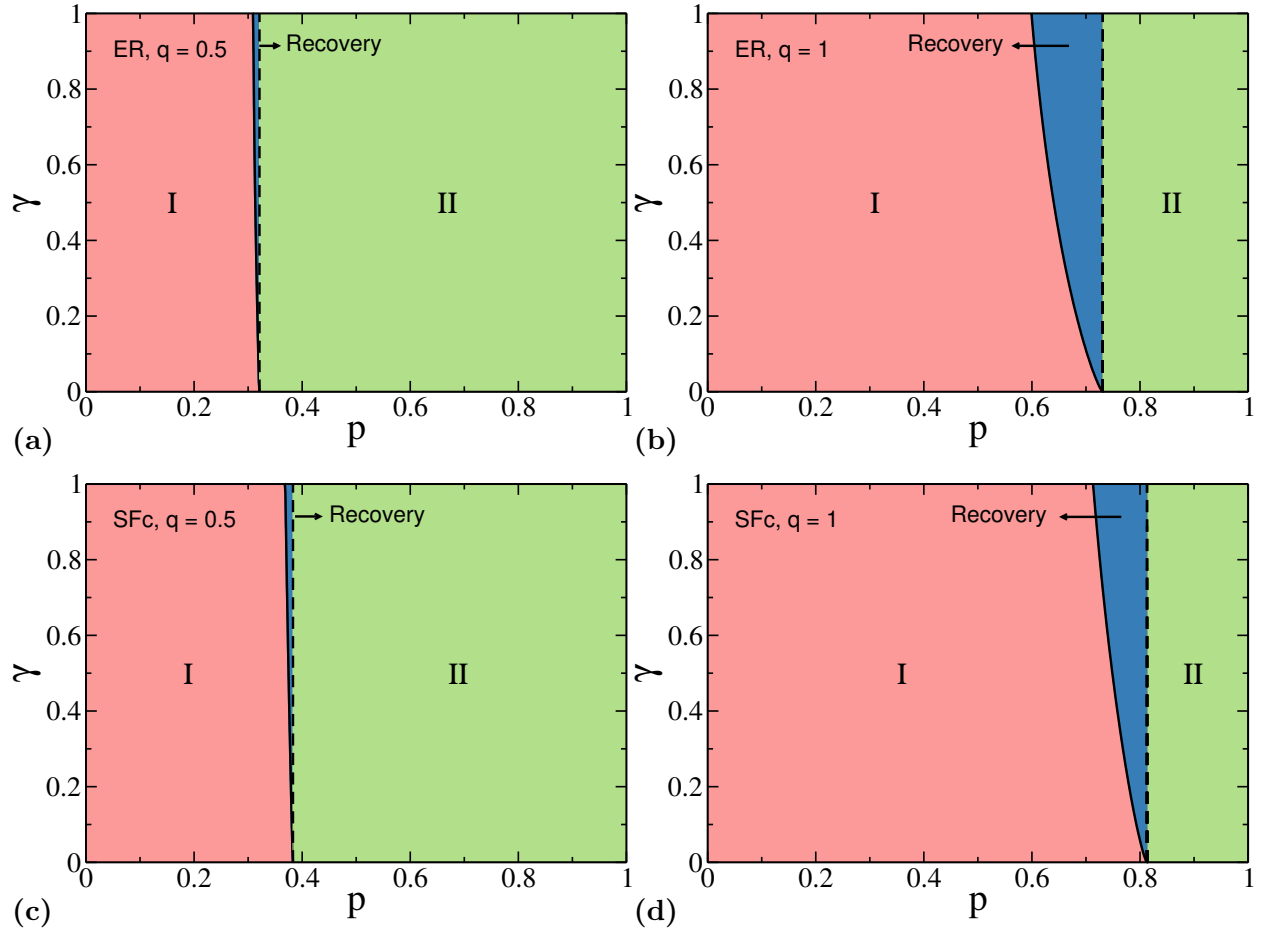


FIG. 7. Phase diagrams on the (p, γ) plane, for the interdependent directed networks analyzed in Fig. 4. The solid lines represent the curves $\gamma_c(p)$ below which the system completely collapses (region I). The dashed lines correspond to the critical point in the absence of the recovery strategy, i.e. $p_c(\gamma = 0)$. Thus, the system would not need a strategy to avoid collapsing to the right of this line (region II). The remaining area is the range of values of $p = p_A(0)$ and γ where the recovery strategy avoids the breakdown and fully restores the system to a functional state.

entirety ($P_\infty = 1$ for $\gamma > 0$). In addition, by observing the phase diagrams it becomes more notorious the effect that the fraction of nodes with dependencies in each network, q , has on the outcome of the cascading process and on the effectiveness that our strategy can achieve. As we commented when analyzing the results from Fig. 4, a smaller value of q (Fig. 7 (a) and (c)) hinders the propagation of failures between networks, because networks become less dependent on each other. However, the region in which the strategy is most useful, avoiding system collapse, is significantly reduced compared to the fully interdependent case, where

$q = 1$ (Fig. 7 (b) and (d)).

Empirical networks

In order to demonstrate the applicability of our model, we simulate the process of cascading failures with recovery of contour nodes in an interdependent system built from an empirical, router-level, communication network [47, 48] obtained from [49]. Since the original network is non-directed, we randomly turn the connections into directed links and work only with the emerging GSCC. Besides, we remove nodes with $k_{in} \leq 1$ or $k_{out} \leq 1$ in order to begin the process with a robust GSCC, as we did with the SFc networks from Fig. 4 (c) and (d). In Fig. 8 (a), we show the degree distribution $P(k)$ before and after modifications. Then, we use the processed network for both layers A and B of our interdependent system, randomly interconnecting nodes from different layers through dependencies and ensuring a fraction q of nodes with dependencies in each network. In Fig. 8 (b), we can observe that the results for the interdependent networks based on empirical data are qualitatively similar to those obtained earlier for synthetic networks.

Contrast with random recovery

Here we present a brief comparison of the proposed recovery strategy with the random repairing of nodes. For this purpose, we simulate cascading failures in the interdependent system based on empirical data (Fig. 8) and compute the amount of recovered nodes throughout the entire process, until the system either collapses or is entirely restored, for both strategies. Note that, for the case $\gamma = 1$, the random recovery strategy repairs all failures at once, restoring the system immediately to a fully functional state, which may be quite unrealistic since usually reparations cannot be implemented everywhere at the same time due to unavailability of resources or technical restrictions. On the other hand, the recovery of contour nodes is implemented on a restricted set of failures, yielding the previously discussed results. Thus, we compare the two strategies in a scenario where the success rate of recovery is $\gamma = 0.5$ and we show the results in Figs. 9 (a) and (b), for $q = 0.5$ and $q = 1$, respectively. We observe that, in both cases, repairing contour nodes requires less resources when compared to the random recovery strategy. This analysis is

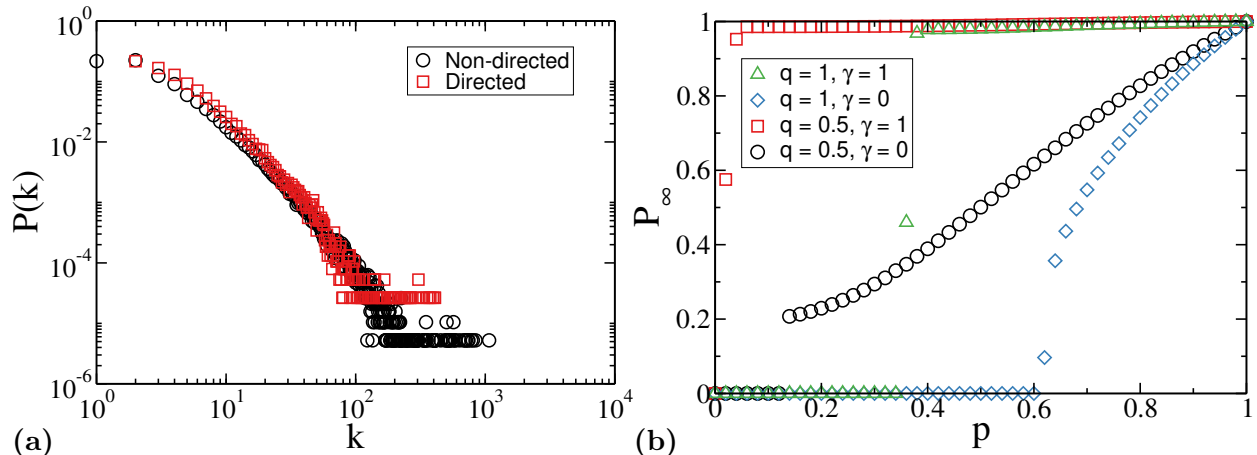


FIG. 8. Application to networks based on empirical data. (a) Degree distribution of the communication network (“tech-RL-caida” obtained from [49]). The original non-directed distribution (circles) has $k_{min} = 1$, $k_{max} = 1071$, and $\langle k \rangle \simeq 6$, while the processed directed network (squares) has $k_{min} = 2$, $k_{max} = 409$, and $\langle k \rangle \simeq 7.7$, for both in and out-degree distributions. The latter represents a directed network of size $N = 37777$, in which all nodes belong to the GSCC. (b) Simulation results for two interdependent networks with the degree distribution of in and out-links described in (a). The results correspond to an average over 10^2 realizations, where interdependencies between networks are randomly assigned.

meaningful for $p > p^*$, with p^* indicated by dashed lines, since below this threshold the system collapses when the strategy that recovers contour nodes is implemented. Below p^* , the random recovery of nodes can restore the system back to a fully functional state, but in doing so it consumes an amount of resources equivalent to more than 1.5 times the size of the entire interdependent system, i.e., $N_{rec} > 3N$, for $q = 0.5$. It is worth mentioning that the random recovery of nodes may waste resources in repairing failures at a given stage of the cascades that will fail again at the next step due to being disconnected from the GSCC of their corresponding network. In this way, the proposed strategy aims to reduce this probability by targeting nodes that, once repaired, become a part of the GSCC.

IV. DISCUSSION

In this paper, we study the effects of implementing a recovery strategy on a process of cascading failures in two interdependent directed networks of the exact same size and

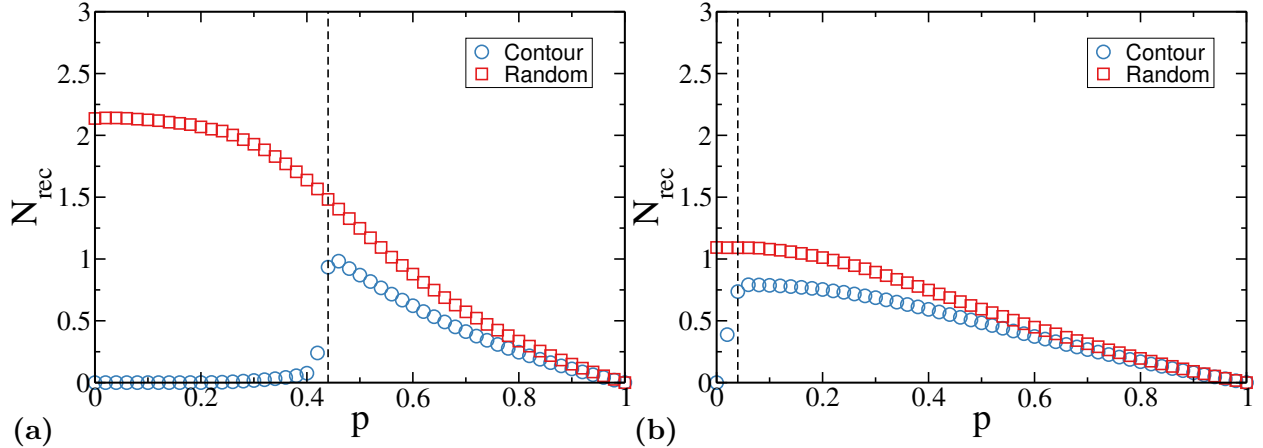


FIG. 9. Fraction of recovered nodes in the final state, N_{rec} , as function of $p = p_A(0)$, for (a) $q = 0.5$ and (b) $q = 1$. The fraction N_{rec} is related to the system size $2N$. Above the threshold p^* (dashed lines), both strategies completely restore the system, but the one that repairs contour nodes requires less amount of resources to do it. The results correspond to an average over 10^2 realizations on the interdependent system built from empirical data and shown in Fig. 8.

degree distributions. In particular, we analyze the scenario in which the fractions of nodes with single dependencies (unidirectional or bidirectional) in each network is q . The strategy consists in repairing, with probability γ , nodes in the contour of the giant strongly connected component (GSCC) of each layer and is implemented immediately after a cascade of failures is triggered by the random removal of a fraction $1 - p$ of nodes in one network. We develop an analytical framework by using node percolation and generating functions, which yield results that are in well agreement with simulations. We find that, if we sustain the strategy until there are no more failures or available nodes to repair, the system undergoes an abrupt transition between a state of full collapse ($P_\infty = 0$) and a state of complete recovery ($P_\infty = 1$). For larger values of q , it is more likely that the strategy helps to avoid collapse in a wider region of the parameter plane (p, γ) . We also find that more homogeneous systems are less vulnerable to cascading failures, as the critical threshold p_c , which defines the abrupt transition, is lower compared to heterogeneous interdependent networks with the same average degree. Finally, we build phase diagrams in the plane (p, γ) by computing the critical values $\gamma_c(p)$ of the recovery probability needed to recover the system. We find three different phases or regions. In the first region, the system collapses even though we intervene with our strategy, thus $P_\infty = 0$ for all values of γ . The second, most interesting phase, is

delimited by the curve $\gamma_c(p)$ and the line $p = p_c(\gamma = 0)$, where $P_\infty = 0$ for $\gamma = 0$ but our strategy achieves the complete recovery of the system, thus $P_\infty = 1$ for $\gamma = 1$. The third region, to the right of the line $p = p_c(\gamma = 0)$, comprehends the most robust phase of the system, where no strategy is needed in order to avoid full collapse, i.e. $P_\infty > 0$ for $\gamma = 0$. Our results are qualitatively similar to those of non-directed interdependent networks [28], although a more detailed comparative analysis would be required in order to establish in which kind of systems the proposed strategy is more or less effective.

Moreover, we demonstrate our model of cascading failures with a recovery strategy in an interdependent system constructed with empirical data of a communication network, and compare the recovery of contour nodes with a random recovery strategy. We find that recovering contour nodes may help in reduce the amount of resources needed in order to restore the functionality of the system. Our findings could serve to inform the development of more robust recovery strategies in real-world infrastructures such as power grids and communication networks. In this way, future research could be focused on including additional features of real infrastructure networks, such as degree correlations of connectivity and dependency links, or improving the recovery strategy by searching nodes outside the contour of each GSCC that, once repaired, can turn back on entire clusters.

V. ACKNOWLEDGMENTS

I. A. P. and C. E. L. wish to thank to UNMdP (EXA 1193/24), FONCyT (PICT 1422/19) and CONICET, Argentina, for financial support. We thank Dr. Lautaro Vassallo for insightful discussions and valuable comments during the preparation of this paper.

Appendix A: Directed network modeling

Considering that an outgoing link, which goes from a source node to a target node, can be viewed as an incoming link from the point of view of the target node and vice-versa, the condition on the average degrees of incoming and outgoing distributions for an isolated network, $\langle k_{in} \rangle = \langle k_{out} \rangle$, must be fulfilled. Then, for each one of the N nodes in the network, we generate random numbers of incoming and outgoing “stubs”, k_{in} and k_{out} , drawn from the corresponding in and out-degree distributions, since the in-degree is not correlated with the

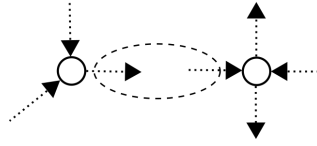


FIG. 10. Configuration model for directed networks. The left node has been assigned $k_{in} = 2$ and $k_{out} = 1$ stubs, while the right nodes has $k_{in} = 2$ and $k_{out} = 2$ stubs, all represented by dotted lines. To form a link, the in and out stubs inside the dashed ellipse were picked at random.

out-degree. By randomly selecting pairs of in and out-stubs from different nodes, we form directed edges (see Fig. 10) while avoiding bidirectional, multiple, and self-links. As well as in non-directed networks, this method yields both uncorrelated incoming and outgoing degrees. We can only successfully match all stubs if $\sum k_{in} = \sum k_{out}$, but for large systems the numbers of in and out-stubs tend to differ. In order to build the networks in a reasonable amount of time, we set a maximum tolerance of 10% for this difference.

Appendix B: Finite clusters

In order to compute the relative size of the finite clusters in both networks at time t , $FC_A(t)$ and $FC_B(t)$, we follow the evolution of the corresponding GSCC, which is the most accurate magnitude in our calculations. For instance, in network A prior to the arrival of B-failures from time step $t - 1$, the real fraction of functional nodes is $\overline{P_\infty^A}(t - 1)$, from which we take away the failures produced by nodes in the FC_B , $FC_B(t - 1) \left[q_A q_B + q_A(1 - q_B) \overline{P_\infty^A}(t - 1) \right]$, resulting in an alternative fraction of remaining nodes in A (different to $p_A(t)$). Then, we obtain $FC_A(t)$ by additionally subtracting the fraction of functional nodes in the $GSCC_A$,

$$FC_A(t) = \overline{P_\infty^A}(t - 1) - FC_B(t - 1) \left[q_A q_B + q_A(1 - q_B) \overline{P_\infty^A}(t - 1) \right] - P_\infty^A(t).$$

Note that the first term of the failures subtracted from $\overline{P_\infty^A}(t - 1)$ corresponds to nodes in FC_B that have a dependency on and provide support to the same node from $GSCC_A$, the only kind of nodes with which nodes in FC_B can have mutual or bidirectional dependencies, which occurs with probability $q_A q_B$. The proportion of failures from FC_B that do not have dependencies but provide support nodes in $GSCC_A$ are captured by the second term, $q_A(1 - q_B) \overline{P_\infty^A}(t - 1)$, which is proportional to $\overline{P_\infty^A}(t - 1)$ as this kind of failures from FC_B can

also provide support already failed A-nodes. The corresponding analysis for the calculation of $FC_B(t)$ is similar, although it involves finite clusters in A at time t rather than $t - 1$,

$$FC_B(t) = \overline{P_\infty^B}(t - 1) - FC_A(t) \left[q_A q_B + q_B (1 - q_A) \overline{P_\infty^B}(t - 1) \right] - P_\infty^B(t).$$

-
- [1] S. Rinaldi, J. Peerenboom, and T. Kelly, *IEEE Cont. Syst.* **21**, 11 (2001).
 - [2] V. Rosato, L. Issacharoff, F. Tiriticco, S. Meloni, S. D. Porcellinis, and R. Setola, *Int. J. Crit. Infrastruct.* **4**, 63 (2008).
 - [3] A. Vespignani, *Nature* **464**, 984 (2010).
 - [4] A. Bashan, Y. Berezin, S. Buldyrev, and S. Havlin, *Nat. Phys.* **9**, 667 (2012).
 - [5] C. D. Brummitt, R. M. D’Souza, and E. A. Leicht, *PNAS* **109**, E680 (2011).
 - [6] S. Boccaletti, G. Bianconi, R. Criado, C. del Genio, J. Gómez-Gardeñes, M. Romance, I. Sendiña-Nadal, Z. Wang, and M. Zanin, *Phys. Rep.* **544**, 1 (2014).
 - [7] M. Kivelä, A. Arenas, M. Barthelemy, J. P. Gleeson, Y. Moreno, and M. A. Porter, *J. Complex Netw.* **2**, 203 (2014).
 - [8] G. D’Agostino and A. Scala, *Networks of Networks: The Last Frontier of Complexity*, Understanding Complex Systems (Springer International Publishing, 2014).
 - [9] L. D. Valdez, L. Shekhtman, C. E. La Rocca, X. Zhang, S. V. Buldyrev, P. A. Trunfio, L. A. Braunstein, and S. Havlin, *J. Complex Netw.* **8** (2020).
 - [10] W. H. Dutton and L. Rohland, WEF (2024), <https://www.weforum.org/agenda/2024/07/global-outage-it-cyber-resilience-alarm-world/> (accessed 27 September 2024).
 - [11] W. M. Leavitt and J. J. Kiefer, *Public Works Manag. Policy* **10**, 306 (2006).
 - [12] M. Sforna and M. Delfanti, in *IEEE PES PSCE* (2006) pp. 301–308.
 - [13] S. Buldyrev, R. Parshani, G. Paul, H. Stanley, and S. Havlin, *Nature* **464**, 1025 (2010).
 - [14] D. Stauffer and A. Aharony, *Introduction to Percolation Theory* (Taylor & Francis, 1994).
 - [15] D. S. Callaway, M. E. J. Newman, S. H. Strogatz, and D. J. Watts, *Phys. Rev. Lett.* **85**, 5468 (2000).
 - [16] R. Parshani, S. V. Buldyrev, and S. Havlin, *Phys. Rev. Lett.* **105**, 048701 (2010).
 - [17] R. Parshani, C. Rozenblat, D. Ietri, C. Ducruet, and S. Havlin, *Europhys. Lett.* **92**, 68002 (2011).

- [18] J. Gao, S. V. Buldyrev, S. Havlin, and H. E. Stanley, *Phys. Rev. Lett.* **107**, 195701 (2011).
- [19] X. Huang, J. Gao, S. V. Buldyrev, S. Havlin, and H. E. Stanley, *Phys. Rev. E* **83**, 065101 (2011).
- [20] G. Dong, J. Gao, R. Du, L. Tian, H. E. Stanley, and S. Havlin, *Phys. Rev. E* **87**, 052804 (2013).
- [21] C. Schneider, N. Yazdani, N. Araujo, S. Havlin, and H. Herrmann, *Sci. Rep.* **3**, 1969 (2013).
- [22] L. D. Valdez, P. A. Macri, and L. A. Braunstein, *J. Phys. A: Math. Theor.* **47**, 055002 (2014).
- [23] G. Dong, Y. Chen, F. Wang, R. Du, L. Tian, and H. E. Stanley, *Chaos* **29**, 073107 (2019).
- [24] G. Dong, F. Wang, L. M. Shekhtman, M. M. Danziger, J. Fan, R. Du, J. Liu, L. Tian, H. E. Stanley, and S. Havlin, *PNAS* **118**, e1922831118 (2021).
- [25] M. Gong, M. Lijia, Q. Cai, and L. Jiao, *Sci. Rep.* **5**, 8439 (2015).
- [26] F. Hu, C. H. Yeung, S. Yang, W. Wang, and A. Zeng, *Sci. Rep.* **6**, 24522 (2016).
- [27] C. E. La Rocca, H. E. Stanley, and L. A. Braunstein, *Physica A* **508**, 577 (2018).
- [28] M. Di Muro, C. La Rocca, H. Stanley, S. Havlin, and L. Braunstein, *Sci. Rep.* **6** (2015).
- [29] D. Bienstock and A. Verma, *SIAM J. Optim.* **20**, 2352 (2010).
- [30] D. Bienstock, in *50th IEEE Conf. Decis. Cont. and Eur. Cont. Conf.* (2011) pp. 2166–2173.
- [31] J. Cohen, F. Briand, and C. Newman, *Community food webs: data and theory*, Biomathematics (Springer Verlag, 1990).
- [32] D. J. Watts and S. H. Strogatz, *Nature* **393**, 440 (1998).
- [33] D. Fell and A. Wagner, *Nat. Biotechnol.* **18**, 1121 (2000).
- [34] H. de Jong, *J. Comput. Biol.* **9**, 67 (2002).
- [35] A. Broder, R. Kumar, F. Maghoul, P. Raghavan, S. Rajagopalan, R. Stata, A. Tomkins, and J. Wiener, *Comput. Netw.* **33**, 309 (2000).
- [36] M. E. J. Newman, S. H. Strogatz, and D. J. Watts, *Phys. Rev. E* **64**, 026118 (2001).
- [37] S. N. Dorogovtsev, J. F. F. Mendes, and A. N. Samukhin, *Phys. Rev. E* **64**, 025101 (2001).
- [38] N. Schwartz, R. Cohen, D. ben Avraham, A.-L. Barabási, and S. Havlin, *Phys. Rev. E* **66**, 015104 (2002).
- [39] X. Liu, H. E. Stanley, and J. Gao, *PNAS* **113**, 1138 (2016).
- [40] X. Liu, L. Pan, H. E. Stanley, and J. Gao, *Phys. Rev. E* **99**, 012312 (2019).
- [41] W. Xu, L. Pan, and X. Liu, *Europhys. Lett.* **133**, 68004 (2021).
- [42] M. Lv, L. Pan, and X. Liu, *Physica A* **620**, 128761 (2023).

- [43] M. Molloy and B. Reed, *Random Struct. Algor.* **6**, 161 (1995).
- [44] M. Boguñá and M. A. Serrano, *Phys. Rev. E* **72**, 016106 (2005).
- [45] J. Gao, S. Buldyrev, H. Stanley, and S. Havlin, *Nat. Phys.* **8**, 40 (2011).
- [46] R. Parshani, S. V. Buldyrev, and S. Havlin, *PNAS* **108**, 1007 (2011).
- [47] N. Spring, R. Mahajan, and D. Wetherall, in *ACM SIGCOMM Comp. Com.*, Vol. 32 (ACM, 2002) pp. 133–145.
- [48] R. A. Rossi, S. Fahmy, and N. Talukder, in *IFIP Networking* (2013) pp. 1–9.
- [49] R. A. Rossi and N. K. Ahmed, in *AAAI* (2015).